

The Growth of Multilayer Graphene over MCM-41 by CVD Method in Atmospheric Pressure: metal-Free Nanocatalyst

Majid Masoumi^{1*}, Ali Morad Rashidi², Mohammadmehdi Choolaei¹, Saeed Sadeghpour¹

¹ Petroleum Refining Division, Research Institute of Petroleum Industry (RIPI), West Blvd. Azadi Sport Complex, P.O. Box 14665-1998, Tehran, Iran

² Nanotechnology Research Center, Research Institute of Petroleum Industry (RIPI), West Blvd. Azadi Sport Complex, Tehran, Iran

Received: 2017-8-02

Accepted: 2017-10-04

Published: 2017-12-20

ABSTRACT

Graphene films were fabricated over synthesized MCM-41 nanocatalyst by chemical vapor deposition method, and the reaction was carried in atmospheric pressure at 750°C. Acetylene gas used as a carbon precursor and the synthesis reaction took place in hydrogen atmosphere. Mesoporous MCM-41 was synthesized at room temperature, using wet chemical method. The synthesized metal free catalyst was characterized by XRD and N₂ adsorption isotherms. The catalytically synthesized graphene layers were characterized by Raman spectroscopy, scanning electron microscopy (SEM), and transmission electron microscopy (TEM). The results indicated that the favorable effect of MCM-41 with high BET surface area (908.76 m²/g) as an active metal free nanocatalyst for fabricating graphene layers with high level of purity and homogeneity. Because of simplicity, easy purification, and high yield of graphene synthesis offered by this method, it is possible to use it in larger scales.

Keywords: Graphene, CVD method, Nanocatalyst, MCM-41.

© 2017 Published by Journal of Nanoanalysis.

How to cite this article

Masoumi M, Rashidi AM, Choolaei M, Sadeghpour S. The Growth of Multilayer Graphene over MCM-41 by CVD Method in Atmospheric Pressure: metal-Free Nanocatalyst. J. Nanoanalysis., 2017; 4(4): 307-312. DOI: [10.22034/jna.2018.545295.1044](https://doi.org/10.22034/jna.2018.545295.1044)

INTRODUCTION

Among different polymorphs of carbon, graphene with fascinating properties, such as high surface area (2630 m²/g) [1], fast charged carrier mobility (~200000 cm²V⁻¹s⁻¹), high thermal conductivity (~5000 W/mK) [2], and strong Young's modulus (~1TPa) [3], has become an interesting target for a considerable number of scientific research [4-6]. Between the different techniques of graphene synthesis, CVD is the most attractive method, because it has some advantages like simple process and the ability of producing

good quality graphene sheets [7], and Transition metals are main catalysts which used extensively in this process [8]. Shu Ye et al synthesize large area graphene sheets over a Cu foil by chemical vapor deposition method in the atmospheric pressure [9].

In another work, Adeniyi Olugbenga Osikoya et al., used acetylene (C₂H₂) as carbon precursor in argon (Ar) and nitrogen (N₂) atmosphere at 850°C for deposition of graphene sheets on 1.00 mm thick copper sheet [10]. Campos-Delgado et al. have reported synthesize of graphene films by CVD from alcohol precursors at atmospheric pressure condition and a highly diluted mixture of Ar-H₂. Their results indicated that the production of mono-

* Corresponding Author Email: masoumim@ripi.ir

and highly decoupled bi-layer graphene films using a simple method [11]. Yakun Chen et al, used Nano Cu powder and polymethylmethacrylate (PMMA) as catalyst and carbon source respectively to fabricate three-dimensional graphene network through chemical vapor deposition method [12].

In another study, Patrick Zeller et al, synthesized graphene in an ultra high vacuum(UHV) chamber at 750°C on single crystalline Ni films on Si wafers by CVD technique under ethylene pressures between 1.3×10^{-8} and 6.7×10^{-8} bar for 2 h [13]. Yunzhou Xue, have used CVD method to fabrication of few-layer graphene sheets on iron catalyst from methane and hydrogen mixture [14].

In another investigation, Murata et al, have reported the growth of monolayer graphene on Palladium catalyst [15]. Arjun Dahal et al. demonstrated the growth of bilayer graphene on Ni (111) thin-film substrate above 650°C [16]. In addition, Li Yinying et al, introduced monolayer graphene synthesis process with Pt foils [17].

Abdul Razak et al. have investigated a new CVD method by introducing direct current during thermal CVD. They have concluded that the additional current in thermal CVD will lead to better control of multilayer graphene growth for interconnect applications [18].

In particular, CVD method has been used widely to synthesize graphene on various substrates, such as Cobalt, Nickel, Platinum, Palladium, Rubidium, Copper, Iron, SiO₂, and SiC. Dependency of these methods to surface properties of substrates and involving difficult experimental procedures, and advanced instrumentation were limited their application for large scale applications [19-21]. Also, the low graphene synthesis yield (i.e., 50 mg of graphene sheet/500 mg of catalyst) of current CVD processes is another barrier to large-scale production of graphene [22].

Mesoporous molecular sieves are one of the interested catalyst supports for different chemical reactions specially carbon nanomaterial synthesis. This attention is due to their special properties, such as large surface area, pore size distribution, pore volume, and easy surface fictionalization. In many investigations, pure siliceous MCM-41 was used as catalyst support for transition metals. The metal-containing MCM-41 such as Co-MCM-41, Ni-MCM-41, Fe-Co-MCM-41 used as catalytic template for the synthesis of CNTs and graphene [23-26].

In this work, metal-free catalyst and cost-

efficient methods were used to grow high quality graphene sheets. These layers were directly synthesized over MCM-41 as nanocatalyst, using CVD method at atmospheric pressure and relatively low temperature for the first time. The synthesized graphenes have been characterized by Raman spectroscopy, SEM and TEM analysis, confirming the formation of graphene layers over MCM-41 template. Fabrication of graphene layers with high level of purity and homogeneity without using any metallic compounds was offered in this investigation. Because of simplicity, easy purification, and high yield of graphene synthesis offered by this method, it is possible to use it in larger scales.

MATERIALS AND SYNTHESIS

Synthesis and purification of MCM-41

In the first step, 70 g of Na₂SiO₃·9H₂O purchased from Merck, was dissolved in 450 ml of distilled water. Then, 1.4763 L C₃H₇NO (Merck) and 54.66 g of a surfactant, N-cetyl-N,N,N-trimethyl ammonium bromide (CTAB) (Merck), were dissolved in 400 ml of distilled water while stirring for around 15 minutes. The second step, the solution of CTAB and C₃H₇NO was then added to the clear solution of silicate, at room temperature (25°C). The reaction mixture was maintained at 25°C for 3 h, then 400 ml of 70% ethanol and 10 ml of 37% HCl were added to the sample and stirred slightly for 30 minutes. At the pH close to 11.0, the yield of MCM41 formation according to Si balance was 71.9%. The surfactants were removed by calcinations at 570°C for 8 h [27, 28].

Synthesis and purification of graphene

Chemical vapor deposition method was carried out in a quartz tube with 45mm diameter and 1 m length, which was placed in a horizontal furnace. The prepared MCM-41 was used as nanocatalyst for synthesis of graphene. At first, 1 g of the catalyst was placed on a quartz boat inside the quartz tube and was purged in nitrogen gas with 300 ml/min flow rate for 30 min and then hydrogen stream with 300 ml/min flow rate to prepare suitable atmosphere for CVD reaction inside the reactor. After that, the reaction was started by acetylene as the carbon source with 30 ml/min flow rate and hydrogen as the carrier gas with 300 ml/min flow rate. The CVD reaction was continued in atmospheric pressure for 30 min at 750°C, and the final product, including the black deposited carbon

materials and catalyst were weighted and purified. The percentage of deposited carbon materials on the MCM-41 catalyst were calculated by the Eq.1 and the result is presented in the Table1.

Carbon deposition yield (%)

$$= \left(\frac{M_T - M_{Cat}}{M_{Cat}} \right) \times 100 \quad \text{Eq.1}$$

Where M_{Cat} is the weight of the catalyst before graphene synthesis and M_T is the weight of final products.

In order to obtain purified carbon materials, the catalyst phase (MCM-41) was removed by treating the solid mixture with 47% HF at ambient temperature for 10 minutes. In order to eliminate carbonaceous impurities, filtered carbon materials were placed in a furnace at 400°C for 2 hours. One of the advantages of graphene synthesis over this metal free nanocatalyst is that the easier purification method in comparison to using metallic catalysts. In this method, there is no need to further acid treating (with HCl or HNO₃) to remove metal particles. The graphene layers deposition yield related to the mass of deposited carbons was calculated from the Eq.2.

Graphene deposition yield (%)

$$= \left(\frac{M_G}{M_T - M_{Cat}} \right) \times 100 \quad \text{Eq.2}$$

Where M_G is the weight of graphene layers after purification. In addition the yield of the purified graphene layers synthesis depends on the mass of MCM-41 catalyst was calculated by the Eq.3.

Graphene synthesis yield (%)

$$= \left(\frac{M_G}{M_{Cat}} \right) \times 100 \quad \text{Eq.3}$$

Characterization methods of materials

Philips PW1848 diffractometer using nickel-filtered Cu K α radiation ($\lambda=0.154$ nm) was used to obtain the X-ray diffraction (XRD) pattern of the synthesized MCM-41 with 2θ range of 0–10° in the steps of 0.02°. Micromeritics ASAP-2010 porosimeter was used to measure the surface area, pore volume and pore size distribution via nitrogen adsorption at 77 K. Pore size distribution (PSD) of the calcined MCM-41 was obtained from adsorption isotherms using Brunauer Emmett Teller (BET) equation. Raman spectra were recorded with a Renishaw Ramanscope in the backscattering configuration using 514.5 nm laser wavelengths. In order to verify the desired structure of the synthesized graphene, Scanning Electron Microscopy (SEM) and Transmission Electron Microscopy (TEM) images were taken using Camscan MV2300 (operating voltage of 15 kV) and JEOL 1200 EXII microscopes (operating voltage of 100 k), respectively.

Table1. Deposition carbon and graphene yields on MCM-41

Catalyst	M_{Cat} (g)	M_T (g)	M_G (g)	Carbon Deposition yield	Graphene deposition yield	Graphene synthesis yield
MCM-41	1.00	1.87	0.31	87%	36%	31%

Table 2. BET surface area, average pore size diameter and pore volume of synthesized MCM-41

Catalyst	BET Surface Area (m ² /g)	Average Pore Diameter (nm)	BET pore volume (cm ³ /g)
MCM-41	908.76	2.88	0.77

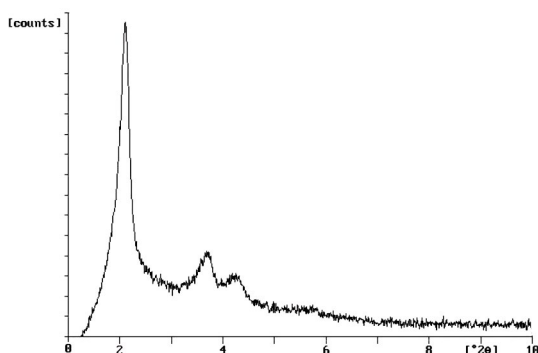


Fig.1. XRD pattern of MCM-41.

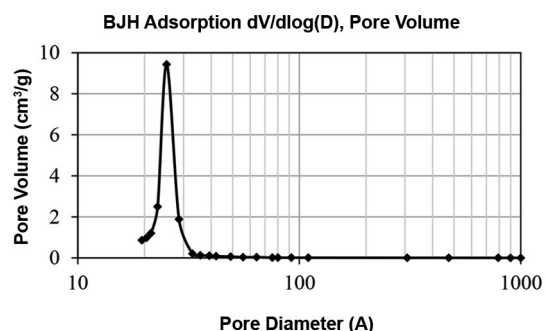


Fig. 2. Pore size distribution of MCM-41.

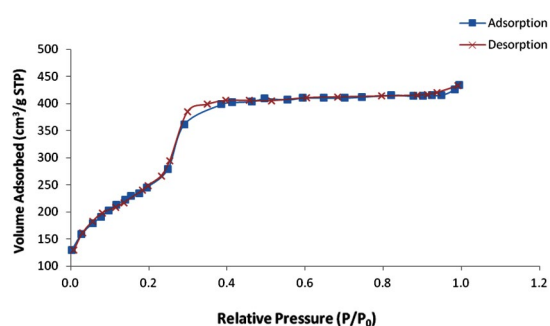
RESULT AND DISCUSSION

Characterization of synthesized MCM-41 catalyst

Figure 1 illustrates the XRD pattern of calcined MCM-41, exhibiting an intense peak of (100) reflection in the range of $1.8^\circ < 2\theta < 2.8^\circ$, and two low intense peaks due to (110) and (200) reflections in the range of $3.8^\circ < 2\theta < 4.8^\circ$. These reflections indicate the formation of well ordered materials with hexagonal structure. In addition, the presence of the related peaks for MCM-41 after calcination indicates the considerable thermal stability of the synthesized MCM-41 [29, 30].

The BET surface area, average pore size diameter and pore volume of the catalyst are presented in Table 2. Figures 2 and 3 respectively represent the PSD and N_2 adsorption–desorption isotherms of the synthesized MCM-41. The observed peak at a pore diameter of 25.2 Å (Figure 2) reveal a pore volume of almost $0.77 \text{ cm}^3/\text{g}$. In addition, the BET surface area of the calcined catalyst was about $908.76 \text{ m}^2/\text{g}$.

The N_2 adsorption–desorption graph (Figure.3) can be divided into different zones: p/p_0 of ≈ 0.3 , $p/p_0 < 0.3$ and $p/p_0 > 0.4$. A sharp inflection step at p/p_0 of ≈ 0.3 depicts the capillary condensation within uniform mesopores. The related isotherms to $p/p_0 < 0.3$ show the monolayer adsorption of N_2 on the pore walls, while those with $p/p_0 > 0.4$ illustrate the multilayer adsorption on the external surface of the particles. The mentioned isotherms indicate type IV character, which is considered as a usual shape for mesoporous MCM-41 [31–33].

Fig. 3. N_2 adsorption–desorption isotherms of MCM-41.

Characterization of synthesized graphene

In order to study the presence and structural characterization of the synthesized graphene, Raman spectroscopy was used as a nondestructive technique. As it can be observed from figure 4, the Raman spectra of the grown graphene over MCM-41 catalyst illustrates three peaks at 1353 cm^{-1} , 1583 cm^{-1} , and 2714 cm^{-1} , respectively related to D, G, and 2D peaks. The D band peak (1353 cm^{-1}) depicts the available structural defects in the analyzed sample [34]. Where, the G-band observed at 1500 cm^{-1} corresponds to the Raman allowed phonon E_{2g} (vibration) mode at the zone centre common to sp^2 carbon materials [35]. The integrated intensity ratio ($I_D/I_G \approx 0.3$) of the D peak along with the considerable G peak illustrates the graphitization of the synthesized graphene with good quality [36].

According to the work done by Subrahmanyam et al., the I_{2D}/I_G intensity ratio is related to the number of graphene layers [37]. A broader 2D peak along with a more pronounced G peak illustrates an

increase in the number of layers of the synthesized graphene. Generally, there are three different borders defined for I_{2D}/I_G value, i.e. $I_{2D}/I_G > 2$ for monolayer graphene, $1 < I_{2D}/I_G < 2$ for bilayer graphene, and $I_{2D}/I_G < 1$ for trilayer graphene [38]. In this regard, the 0.6 value for I_{2D}/I_G (resulting from figure 4) indicates a trilayer structure for the synthesized graphene.

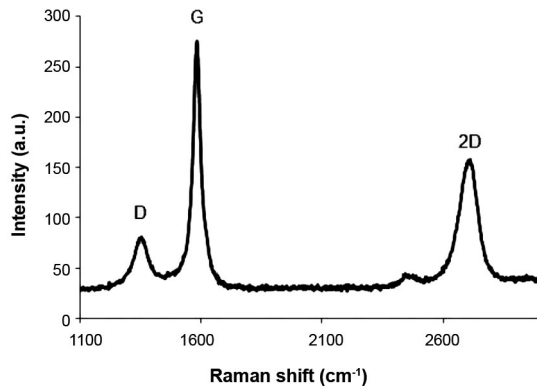


Fig. 4. Raman spectroscopy of purified graphene layers.

Figure 5 shows the pore size distribution of synthesized graphene layers. The final structure of the synthesized graphene sheets were evaluated using SEM images (figure 6). The SEM image clearly indicates the continuous graphene layers synthesized over MCM-41 nano-catalytic template with a number of wrinkles. In addition, the detailed morphology of the graphene layers was further studied using TEM image (figure 7). The TEM images indicate the absence of amorphous and microcrystalline carbon along with the high level of purity and homogeneity of the graphene layers. The SEM and TEM results confirm the positive influence of pure MCM-41 as an active catalyst for graphene fabrication.

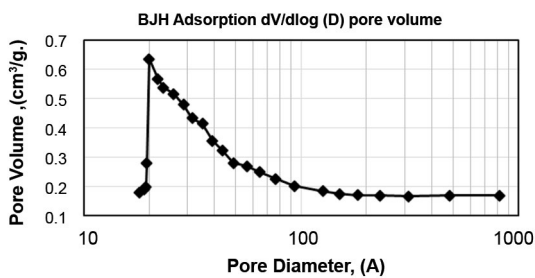


Fig. 5. Pore size distribution of graphene.



Fig. 6. SEM image of the graphene layers over MCM-41 catalyst.

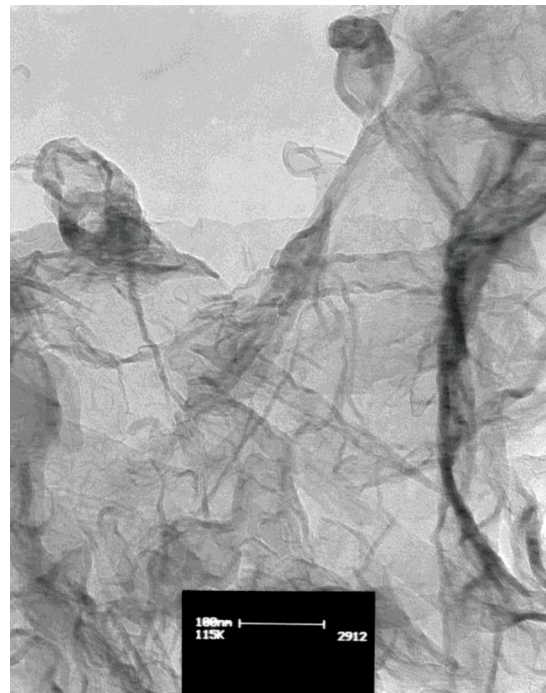


Fig. 7. TEM images of the synthesized graphene.

CONCLUSION

Graphene layers were successfully synthesized

through a metal free catalyst and cost-efficient atmospheric CVD method directly over MCM-41 nanocatalyst. The reaction temperature was fixed at 750°C and acetylene was used as the carbon source. Fabrication of well ordered MCM-41 with hexagonal structure was confirmed by XRD and N₂ adsorption isotherms. The results of N₂ adsorption isotherms also revealed a pore volume and BET surface area of about 0.77 cm³/g and 908.76 m²/g, respectively. The successful synthesis of catalytically produced graphene layers was confirmed by Raman spectroscopy, SEM, and TEM techniques. Moreover, the high yield of graphene synthesis over MCM-41 along with the suitable integrated intensity ratio (I_D/I_G=0.3) indicate the high activity of the synthesized catalyst and considerable capability of the proposed technique for graphene fabrication.

CONFLICT OF INTEREST

The authors declare that there is no conflict of interests regarding the publication of this manuscript.

REFERENCES

- M.D. Stoller, S. Park, Y. Zhu, J. An, and R.S. Ruoff. *Nano Lett.* 8, 3498-3502 (2008).
- A.A. Balandin, S. Ghosh, W. Bao, I. Calizo, D. Teweldebrhan, F. Miao, and C.N. Lau. *Nano Lett.* 8, 902-907 (2008).
- C. Lee, X. Wei, J.W. Kysar, and J. Hone. *Science* 321, 385-388 (2008).
- K.S. Novoselov, A.K. Geim, S.V. Morozov, D. Jiang, Y. Zhang, S.V. Dubonos, I.V. Grigorieva, and A.A. Firsov. *Science* 306, 666-669 (2004).
- I.A. Luk'yanchuk and Y. Kopelevich. *Phys. Rev. Lett.* 93, 166402 (2004).
- K.S. Novoselov, Z. Jiang, Y. Zhang, S.V. Morozov, H.L. Stormer, U. Zeitler, J.C. Maan, G.S. Boebinger, P. Kim, and A.K. Geim. *Science* 315, 1379-1379 (2007).
- G. Wang, M. Zhang, Y. Zhu, G. Ding, D. Jiang, Q. Guo, S. Liu, X. Xie, P.K. Chu, and Z. Di. *Sci. Rep.* 3, 2465 (2013).
- X. Chen, L. Zhang, and S. Chen. *Synth. Met.* 210, 95-108 (2015).
- S. Ye, K. Ullah, L. Zhu, A. Ali, W.K. Jang, and W.-C. Oh. *Solid State Sci.* 46, 84-88 (2015).
- A.O. Osikoya, O. Parlak, N.A. Murugan, E.D. Dikio, H. Moloto, L. Uzun, A.P.F. Turner, and A. Tiwari. *Biosens. Bioelectron.* 89, 496-504 (2017).
- J. Campos-Delgado, A.R. Botello-Méndez, G. Algara-Siller, B. Hackens, T. Pardo, U. Kaiser, M.S. Dresselhaus, J.-C. Charlier, and J.-P. Raskin. *Chem. Phys. Lett.* 584, 142-146 (2013).
- Y. Chen, X. Zhang, E. Liu, C. He, Y. Han, Q. Li, P. Nash, and N. Zhao. *J. Alloys Compd.* 688, 69-76 (2016).
- P. Zeller, A.-K. Henß, M. Weinl, L. Diehl, D. Keefer, J. Lippmann, A. Schulz, J. Kraus, M. Schreck, and J. Wintterlin. *Surf. Sci.* 653, 143-152 (2016).
- Y. Xue, B. Wu, Y. Guo, L. Huang, L. Jiang, J. Chen, D. Geng, Y. Liu, W. Hu, and G. Yu. *Nano Res.* 4, 1208-1214 (2011).
- Y. Murata, E. Starodub, B.B. Kappes, C.V. Ciobanu, N.C. Bartelt, K.F. McCarty, and S. Kodambaka. *Appl. Phys. Lett.* 97, 143114 (2010).
- A. Dahal, R. Addou, P. Sutter, and M. Batzill. *Appl. Phys. Lett.* 100, 241602 (2012).
- L. Yinying, W. Xiaoming, W. Huaqiang, and Q. He. *J. Semicond.* 36, 013005 (2015).
- L.A. Razak, D. Tobino, and K. Ueno. *Microelectronic Engineering* 120, 200-204 (2014).
- L. Gao, J.R. Guest, and N.P. Guisinger. *Nano Lett.* 10, 3512-3516 (2010).
- Y. Gong, X. Zhang, G. Liu, L. Wu, X. Geng, M. Long, X. Cao, Y. Guo, W. Li, J. Xu, M. Sun, L. Lu, and L. Liu. *Adv. Funct. Mater.* 22, 3153-3159 (2012).
- Z. Peng, F. Somodi, S. Helveg, C. Kisielowski, P. Specht, and A.T. Bell. *J. Catal.* 286, 22-29 (2012).
- Y. Shen and A.C. Lua. *Sci. Rep.* 3, 3037 (2013).
- R. Atchudan, A. Pandurangan, and J. Joo. *Microporous Mesoporous Mater.* 175, 161-169 (2013).
- Y. Chen, D. Ciuparu, S. Lim, Y. Yang, G.L. Haller, and L. Pfefferle. *J. Catal.* 225, 453-465 (2004).
- T. Somanathan and A. Pandurangan. *Appl. Surf. Sci.* 254, 5643-5647 (2008).
- Q. Zhao, T. Jiang, C. Li, and H. Yin. *J. Ind. Eng. Chem.* 17, 218-222 (2011).
- M. Hasanzadeh, N. Shadjou, S.-T. Chen, and P. Sheikhzadeh. *Catal. Commun.* 19, 21-27 (2012).
- R. Shahnaz, S. Nasrin, and F. Atena. *Curr. Nanoscience.* 8, 776-782 (2012).
- M. Urbán, D. Méhn, Z. Kónya, and I. Kiricsi. *Chem. Phys. Lett.* 359, 95-100 (2002).
- D. Subashini and A. Pandurangan. *Catal. Commun.* 8, 1665-1670 (2007).
- A. Corma. *Chem. Mater.* 97, 2373-2420 (1997).
- A. Vinu, J. Dědeček, V. Murugesan, and M. Hartmann. *Chem. Mater.* 14, 2433-2435 (2002).
- M. Selvaraj, P.K. Sinha, K. Lee, I. Ahn, A. Pandurangan, and T.G. Lee. *Microporous and Mesoporous Mater.* 78, 139-149 (2005).
- F.T. Si, X.W. Zhang, X. Liu, Z.G. Yin, S.G. Zhang, H.L. Gao, and J.J. Dong. *Vacuum.* 86, 1867-1870 (2012).
- Z. Tu, Z. Liu, Y. Li, F. Yang, L. Zhang, Z. Zhao, C. Xu, S. Wu, H. Liu, H. Yang, and P. Richard. *Carbon.* 73, 252-258 (2014).
- M.A. Pimenta, G. Dresselhaus, M.S. Dresselhaus, L.G. Cancado, A. Jorio, and R. Saito. *PCCP.* 9, 1276-1290 (2007).
- K.S. Subrahmanyam, L.S. Panchakarla, A. Govindaraj, and C.N.R. Rao. *J. Phys. Chem.* 113, 4257-4259 (2009).
- Q. Yu, L.A. Jauregui, W. Wu, R. Colby, J. Tian, Z. Su, H. Cao, Z. Liu, D. Pandey, D. Wei, T.F. Chung, P. Peng, N.P. Guisinger, E.A. Stach, J. Bao, S.-S. Pei, and Y.P. Chen. *Nat Mater.* 10, 443-449 (2011).